Detection of steering direction using EEG recordings based on sample entropy and time-frequency analysis*

Calderó-Bardají, P., Longfei, X., Jaschke, S., Reermann, J., Mideska, K.G., Schmidt, G., Deuschl, G., and Muthuraman, M.

***Abstract*— Monitoring driver's intentions beforehand is an ambitious aim, which will bring a huge impact on the society by preventing traffic accidents. Hence, in this preliminary study we recorded high resolution electroencephalography (EEG) from 5 subjects while driving a car under real conditions along with an accelerometer which detects the onset of steering. Two sensor-level analyses, sample entropy and time-frequency analysis, have been implemented to observe the dynamics before the onset of steering. Thus, in order to classify the steering direction we applied a machine learning algorithm consisting of: dimensionality reduction and classification using principal-component-analysis (PCA) and support-vector-machine (SVM), respectively. The results showed an increase of the sample entropy and the estimated power values in the theta and alpha frequency bands, 100 ms before the onset of steering. The detection of steering direction depicted that sample entropy gives a higher classification accuracy (73.5%±6.8) as compared to that of using the estimated power for theta and alpha frequency bands (62.6%±5.6).**

I. INTRODUCTION

Electroencephalography (EEG) is a key technique in neuroscience with high temporal resolution and low cost which has been commonly used as a diagnostic technique. EEG analyzes the small voltage fluctuations of the brain using electrodes that are usually placed non-invasively on the scalp. More recently, the use of this technique has been extended to other applications which aim in using the information extracted from the EEG recordings while the subject performs certain tasks in order to identify, analyze or further communicate with other devices, also known as brain computer interface (BCI). The applications of BCI are wide, from controlling wheelchairs [1] to spelling by thoughts [2], which can improve the living conditions of people in particular circumstances.

One of the biggest needs in our society is to improve the security in roads and highways. The number of licensed drivers increase every year in almost all countries of the world. This fact has a direct correlation with the increasing number of traffic accidents which in most cases could be prevented. As a result, large number of human losses occur. In addition, other factors rise such as economic losses for the transported assets, insurances or jams.

Our study aims to help in the reduction of human victims and economic losses in roads and highways by implementing a system which monitors driver's intentions. There are different studies which have analyzed EEG signals while driving, achieving successful performances mostly in simulated environments [3] [4]. However, this study is taking a challenge performing the analysis on a natural environment by driving a real car, where complex tasks take place at the same time.

Monitoring drivers has been approached with other techniques such as electromyography (EMG) [5], electrocardiography (ECG) [6] or electrooculography (EOG) [7], as well as integrated sensors for example in the driver pedals [8], or in the seats with contactless sensors [9]. Combining more information would improve the security by recognizing the driver actions even beforehand, making the driving experience more secure and comfortable.

Integrated car systems are already being used, as an example, detecting distances between cars, as well as other objects [10]. There is a high complexity of monitoring drivers because of the variability in physiological signals between subjects and also within subjects from time to time. Thus, designing a system which analyzes robustly and accurately is a required aim in order to transfer this technology to daily applications.

II. DATA ACQUISITION AND PREPROCESSING

We have taken EEG recordings from 5 subjects (25.2±1.5 years) using Geodesic EEG System 300 based on 256 electrodes placed according to the international 10-20 system. All subjects had valid driving license and experience in driving an automatic car. The task took place in an area where no other cars were passing by. The subjects were asked to drive straight until they reached an intersection. Then, the command 'right' or 'left' was randomly given to the driver in order not to get habituated. An accelerometer sensor was attached in the top of the steering wheel, so that, it detected the rotation of the wheel triggering a signal that was used as a marker for the onset of steering. The task was repeated 20 times for each subject. The recording lasted for two and a half hours for each subject including preparation time. The sampling rate was 1 kHz. Some recordings had to be discarded because of experimental problems like bad connections, dryness of the sponge pad of the EEG electrodes

*This work was supported by SFB 855 Project D2.

Calderó-Bardají, P., Longfei, X., Jaschke, S., Reermann, J. and Schmidt, G. are with the Institute for Digital Signal Processing and System Theory, Faculty of Engineering, Christian-Albrechts-University of Kiel, 24105 Kiel, Germany. paucaldero@gmail.com, xionglongfei@hotmail.com, svenjota@.gmail.com, jere@tf.uni-kiel.de, gus@tf.uni-kiel.de

Mideska, K.G. and Deuschl, G. are with the Department of Neurology, Christian-Albrechts-University of Kiel, 24105 Kiel, Germany. kgm@tf.uni-kiel.de, g.deuschl@neurologie.uni-kiel.de

Muthuraman, M. is with the Department of Neurology, Johannes-Gutenberg-University of Mainz, 55131 Mainz, Germany muthuraman.muthuraman@unimedizin-mainz.de

(caused by volatilization of the electrolyte solution) or body movements. The signals from 12 seconds before to 4 seconds after steering were selected for the analyses. Common average referencing was performed on the measured signals [11] in order to capture very small signals before we performed further analysis. Then, we applied a moving average window of size 100 ms.

III. METHODS

The methodology is presented in three parts. The first part describes the sensor-level analyses: sample entropy and time-frequency analysis from the EEG signals. The second part describes dimensionality reduction, whereby we selected first those electrodes corresponding to the region of interest, the motor cortex area, and then combined this information into a reduced number of features by applying principal-component-analysis (PCA). The third part describes classification using support-vector-machine (SVM) with a linear kernel. The performance of the algorithm was evaluated and averaged with a 5-Fold cross validation loop.

A. Sensor-Level Analyses

We analyzed the measured EEG signals in order to reveal information which was not observable in the raw data. Therefore, we chose these two methods to process the EEG signals: sample entropy and time-frequency analysis.

1) Sample Entropy: In information theory, entropy is used as a mathematical measure for randomness. The brain activity detected by the EEG will have a steady pattern for a monotonous activity. Therefore, we had the hypothesis that randomness in EEG signals will increase when changing the activity from driving straight to steering, what was observed calculating sample entropy [12] [13].

An EEG time series of length N can be represented by $u(j) : 1 \leq j \leq N$. We want to form m partial blocks of length $N - m + 1$ from the EEG time series, which are represented by:

$$x_m(i) = u(i+k) \begin{cases} 1 \leq i \leq N - m + 1 \\ 1 \leq k \leq m \end{cases} \tag{1}$$

The next step is to calculate the Chebyshev distance between all combinations of $x_m(i)$, selecting those whose distance is smaller than r, defined as tolerance.

$$d[x_m(i), x_m(j)] = max\big|u(i+k) - u(j+k)\big| \tag{2}$$

The vectors $x_m(j)$ whose $d[x_m(i), x_m(j)] \leq r$ will be introduced to the variable B_i. Normalizing B_i and excluding its self-matches with $j : 1 \leq j \leq N-m \mid j \neq i$, we get B^m.

$$B^m = \frac{N-m-1}{N-m} \sum_{i=1}^{N-m} B_i \tag{3}$$

Repeating the procedure for $m+1$ blocks of the same EEG time series, we get B^{m+1}. Finally, calculating the logarithm of the ratio between B^{m+1} and B^m, we obtain the expression for sample entropy with m, r and N as parameters:

$$SampEn(m, r, N) = -ln \frac{B^{m+1}}{B^m} \tag{4}$$

B^{m+1} will always be smaller than or equal to B^m, therefore getting values equal or greater than zero. We set $m = 2$ and $r = 0.3$.

2) Time-Frequency Analysis: The EEG signal was analyzed in time and frequency domain simultaneously. The mathematical motivation for this analysis was to get a relation between the activity in each frequency band of the EEG [14] and the different time points while driving straight and steering. Therefore we performed the time frequency representation (TFR) based on multitapering of the signal using a Hanning taper [15], to analyze temporally the behavior of the signal power at each frequency.

B. Dimensionality Reduction

Prior to performing the classification algorithm, we selected the results from the sensor-level analyses by restricting our region of interest to be the motor cortex area from both hemispheres, to reduce the number of electrodes. Thus, we selected 75 electrodes which were located in this area and normalized them to zero mean and unity standard deviation to compensate the scaling variabilities. Then, we combined the information of the normalized electrodes reducing the dimensionality by applying PCA.

PCA is a multivariate statistical method based on Karhunen-Loève expansion that we used to reduce the dimensionality from the sensor-level data expressing the information in terms of linear combinations of orthogonal vectors along a new set of coordinates, where the sample variances are uncorrelated. Mathematically, this transformation is described as:

$$Y = W \cdot X, \tag{5}$$

where X is the data, W is the projection matrix and Y represents the orthogonal vectors or principal components (PC). Each PC represents a certain amount of variance in the data, ranked by a decreasing degree. The first PC will carry the largest variance and the last PC the least, usually representing almost no information about the original data.

The more features one can use the more information is available to differentiate between directions. However, more training data are needed in order not to bias the model, what is known as curse of dimensionality [16]. In this case, we selected only the first three to five principal components which carried the highest amount of variance.

C. Classification

To evaluate the separability between features corresponding to different steering directions we used SVM [17]. SVM calculates a decision boundary, in this case to classify the directions of steering, using a hyperplane which achieves the optimal distance between classes. A simple model will have better generalization properties, therefore we assumed linear separability, describing the hyperplane as:

$$\vec{v} \cdot \vec{x} + c = 0, \tag{6}$$

where $\vec{v}$ is an orthogonal vector to the hyperplane, $\vec{x}$ is a vector containing the data and c is a constant. To separate the classes, a hyperplane which validates the inequalities for the data elements from left (L) and right (R) steering direction classes, is given as:

$$\vec{v} \cdot \vec{x_i} + c \geq 1 \text{ for direction L} \tag{7}$$

$$\vec{v} \cdot \vec{x_i} + c \leq -1 \text{ for direction R} \tag{8}$$

Combining equations (7) and (8) gives:

$$y_b(\vec{v} \cdot \vec{x_i} + c) - 1 \geq 0, \tag{9}$$

where y_b is a binary variable equivalent to 1 for direction L and to -1 for direction R. The features from class 1 which satisfy equation (7) determine the hyperplane H_1. The distance between the origin and H_1 is:

$$d_{\mathrm{L}} = \frac{1 - c_{|}}{||\vec{v}||} \tag{10}$$

Similarly for class -1 the distance between the origin and hyperplane H_{-1} is:

$$d_{\mathrm{R}} = \frac{-1 - c_{|}}{||\vec{v}||} \tag{11}$$

As H_1 and H_{-1} are parallel and no training points are located between them, the distance between the hyperplanes or margin is given as:

$$d\big((\vec{v}, c), x_i\big) = \frac{2}{||\vec{v}||} \tag{12}$$

The hyperplane which maximizes d will be the optimal hyperplane. To avoid bias in the results, the data were divided into training and test sets using 5-Fold cross validation. The classifier performance was evaluated with a confusion matrix, yielding sensitivity, specificity and accuracy, defined for our purpose as:

$$Sensitivity = \frac{True\text{ L}}{True\text{ L } + False\text{ R}} \tag{13}$$

$$Specificity = \frac{True\text{ R}}{True\text{ R } + False\text{ L}} \tag{14}$$

$$Accuracy = \frac{True\mathrm{L} + True\mathrm{R}}{True\mathrm{L} + False\mathrm{R} + True\mathrm{R} + False\mathrm{L}} \tag{15}$$

IV. RESULTS

The results from the two sensor-level analyses are shown in Fig. 1 and 2, which depict the change in dynamics between driving straight and steering.

A. Sample Entropy and TFR

As it can be observed in Fig. 1, the results from sample entropy analysis showed an increase before the onset of steering, which was not visible in the raw data.

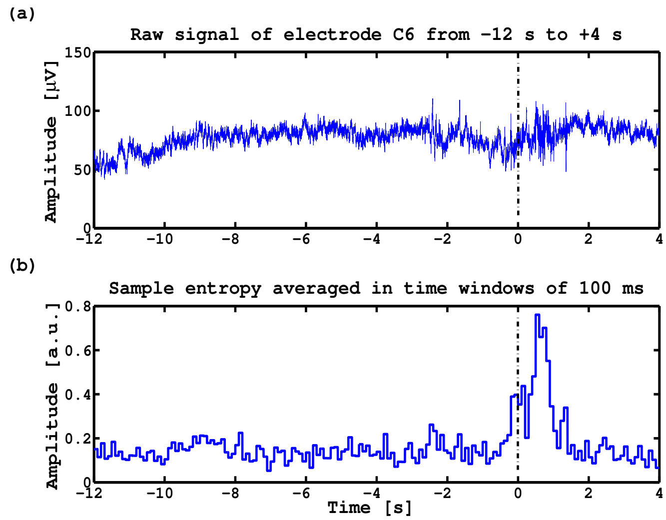

Fig. 1. (a) As an example, EEG signal of electrode C6 from a representative subject while steering to the left (b) Corresponding sample entropy values smoothed by a moving average window of 100 ms. Time point 0 corresponds to the steering onset.

Similarly, the estimated power from the TFR showed an increase in the theta (4-7 Hz) and alpha (8-15 Hz) frequency bands, before the steering onset, as shown in Fig. 2.

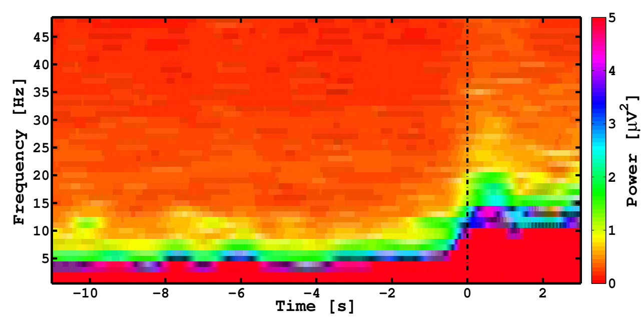

Fig. 2. Time-frequency plot representing an increase in the power dynamics of a representative subject before the onset of steering, smoothed by a moving average window of 100 ms. Time point 0 corresponds to the steering onset.

B. Classification

The extracted features by PCA were classified by SVM with a linear kernel. The dimensionality of the original data was reduced using the PCA sub-dimensional space, hence reducing the complexity of the classifier, as shown in Fig. 3.

The evaluation of the classification in the time window between –100 ms and the onset is shown in Table I for both analyses of each subject separately, where accuracy, sensitivity and specificity are given in percentage. In the case of estimated power, the results are shown for those frequency bands that showed best performance.

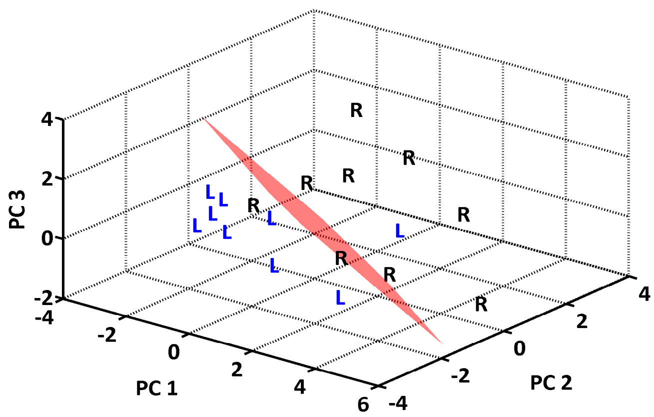

Fig. 3. Visualization of the first 3 principal components from the sample entropy analysis of a representative subject. A hyperplane in the middle shows the separability between the steering directions. Each letter represents a single trial for left (L) or right (R).

TABLE I

PERFORMANCE OF STEERING PREDICTION USING SAMPLE ENTROPY AND ESTIMATED POWER

Subject	**Entropy**			**Estimated Power**			
	Acc	Sens	Spec	Band	Acc	Sens	Spec
1	80	80	80	θ	60	62.5	58
2	63.5	60	67	α	63	62.5	63.5
3	79	73	85	θ	67	67	67
4	75	75	75	θ	69	67	71
5	70	60	80	α	55	43	67
Mean	**73.5**	**69.6**	**77.4**		**62.8**	**60.4**	**65.3**
Std	6.8	9.1	6.8		5.6	10.0	4.9

In total 83 steering repetitions from 5 subjects have been analyzed, where 40 were to the left and 43 to the right direction. As it can be seen, the average performance from the sample entropy showed higher accuracy values compared to the estimated power, ranging from 63.5% to 80%, while for power the accuracies ranged from 55% to 69%.

V. CONCLUSIONS

We have confirmed the feasibility of detecting the steering direction prior to the onset based on the two sensor-level analyses: sample entropy and time-frequency analysis. Driving straight dynamics were distinguishable from steering in both analyses, showing a different activity pattern. The classification gave a better performance for the sample entropy as compared to the estimated power. Our study depicted that it is possible to improve the estimation of driver's steering direction for a larger number of trials per subject, using an adaptive approach by having a parameter selection step after the dimensionality reduction.

The accuracy that we achieved under real environment is comparable to those studies [3] which were performed under simulated environment having different time windows. The detection system used in this study is compatible with other studies on braking prediction or brain state tracing. Integration with other techniques such as EOG or EMG and the corresponding data fusion could improve the performance and robustness of detection. This technique can be applied to smart-cars in combination with driving systems which process the information of the surrounding aiming to improve the security while driving. In the future, an increase in the sample size will allow an increase of estimated parameters for the classification.

ACKNOWLEDGMENT

The authors would like to thank to all the subjects that have participated in the experiments and to the German Research Council (Deutsche Forschungsgemeinschaft, DFG, SFB 855, Project D2).

REFERENCES

[1] F. Galán, M. Nuttin, E. Lew, P.W. Ferrez, G. Vanacker, J. Philips, J.D.R. Millán, A brain-actuated wheelchair: asynchronous and non-invasive braincomputer interfaces for continuous control of robots, Clinical Neurophysiology, 119(9), 2159-2169, 2008.

[2] R. Scherer, G.R. Mueller, C. Neuper, B. Graimann, G. Pfurtscheller, An asynchronously controlled EEG-based virtual keyboard: improvement of the spelling rate, IEEE Transactions on Biomedical Engineering, 51(6), 979-984, 2004.

[3] H. Zhang, R. Chavarriaga, L. Gheorghe, J.D.R. Millán, Inferring driver's turning direction through detection of error related brain activity, Engineering in Medicine and Biology Society, 35th Annual International Conference of the IEEE, 2196-2199, July 2013.

[4] I.H. Kim, J.W. Kim, S. Haufe, S.W. Lee, Detection of braking intention in diverse situations during simulated driving based on EEG feature combination, Journal of Neural Engineering, 12(1), 016001, 2014.

[5] V. Balasubramanian, K. Adalarasu, EMG-based analysis of change in muscle activity during simulated driving, Journal of Bodywork and Movement Therapies, 11(2), 151-158, 2007.

[6] T. Matsuda, M. Makikawa, ECG monitoring of a car driver using capacitively-coupled electrodes, In Engineering in Medicine and Biology Society, 30th Annual International Conference of the IEEE, 1315-1318, August, 2008.

[7] T.C. Chieh, M.M. Mustafa, A. Hussain, S.F. Hendi, B.Y. Majlis, Development of vehicle driver drowsiness detection system using electrooculogram (EOG), In Computers, Communications, & Signal Processing with Special Track on Biomedical Engineering, 165-168), November, 2005.

[8] Y. Kobayashi, T. Kimura, T. Yamamura, G. Naito, Y. Nishida, Development of a prototype driver support system with accelerator pedal reaction force control and driving and braking force control (No. 2006-01-0572). SAE Technical Paper, 2006.

[9] M. Walter, B. Eilebrecht, T. Wartzek, S. Leonhardt, The smart car seat: personalized monitoring of vital signs in automotive applications, Personal and Ubiquitous Computing, 15(7), 707-715, 2011.

[10] J.C. McCall, M.M. Trivedi, Video-based lane estimation and tracking for driver assistance: survey, system, and evaluation, IEEE Transactions on Intelligent Transportation Systems, 7(1), 20-37, 2006.

[11] D.J. McFarland, L.M. McCane, S.V. David, J.R. Wolpaw, Spatial filter selection for EEG-based communication, Electroencephalography and clinical Neurophysiology, 103(3), 386-394, September 1997.

[12] J.S. Richman, J.R. Moorman, Physiological time-series analysis using approximate entropy and sample entropy, American Journal of Physiology-Heart and Circulatory Physiology, 278(6), June 2000.

[13] P. Grassberger, I. Procaccia, Estimation of the Kolmogorov entropy from a chaotic signal, Physical review A, 28(4), 2591, 1983.

[14] D.B. Percival, A.T. Walden, Spectral Analysis for physical applications, Cambridge University Press, 1993.

[15] P.P. Mitra, B. Pesaran, Analysis of dynamic brain imaging data, Biophysical journal, 76(2), 691-708, February 1999.

[16] R.E. Bellman, Dynamic programming and Lagrange multipliers, Proceedings of the National Academy of Sciences, 42(10), 767-769, 1956.

[17] C. Cortes, V.N. Vapnik, Support-vector networks, Machine learning, 20(3), 273-297, 1995.